POLYMORPHISM OF THE MICAS

STERLING B. HENDRICKS,

WITH OPTICAL MEASUREMENTS

MERRILL E. JEFFERSON,

Fertilizer Research Division, Bureau of Chemistry and Soils,
U. S. Department of Agriculture, Washington, D. C.

Many systematic studies have been made of the compositions and optical properties of the micas, but failure of good face development other than the prominent cleavage has limited crystallographic work. Micas have been variously described, without real crystallographic evidence, as monoclinic, hexagonal, and triclinic; the preference usually being for monoclinic. X-ray diffraction patterns of muscovite show that it is monoclinic and the few published results on biotite lead to a similar conclusion.

It has been an objective of this laboratory to obtain structural information on minerals important in determining the properties of soils. The following study, while a part of this program, originated in an entirely accidental manner. One of several biotite samples that were being examined in a study of diffuse scattering from the micas showed an unexpectedly complicated diffraction pattern. A wealth of polymorphism was found upon digressing.

X-ray diffraction patterns were made from single crystals of more than a hundred specimens of micas. Crystal structure analyses were then carried out for the various polymorphic modifications. In presenting the results, however, it is more convenient first to describe the structures, and then to discuss the various specimens.

gave freely of his time in discussion. The best suite of samples available were the lepidolites that had been so carefully analyzed by Mr. R. E. Stevens of the U. S. Geological Survey. Dr. A. F. Hagner, of Columbia University, supplied a large number of samples, only a few of which were studied, and Dr. R. W. Webb, of the University of California at Los Angeles furnished a sample of alurgite that he has recently described. Possible significance of open groups of symmetry operations was discussed with Professor E. Teller, of George Washington University.

General Description of the Mica Structure

A general type of structure shown by many silicate layer minerals, including the micas, was first proposed by Pauling[*1] on the basis of his coordination theory. Mauguin[2] earlier had measured the units of structure and had discussed types of isomorphous replacement. He pointed out that the c-axis of biotite apparently was only half as long as that of muscovite. Jackson and West[3] made a detailed analysis of the structure of muscovite independent of Pauling's work.

The composition of muscovite approximates $[Al_2]$ $(AlSi_3)O_{10}(OH, F)_2K$. Aluminum shown in brackets, $[Al_2]$, has octahedral coordination with respect to neighboring oxygen and hydroxyl ions. It is replaced by magnesium in phlogopite, $[Mg_3]$ $(AlSi_3)O_{10}(OH, F)_2K$, and by magnesium, lithium, titanium, ferric and ferrous iron in various other micas related to biotite and lepidolite. An atom of a group $(AlSi_3)$ is surrounded by four oxygen ions at the corners of a tetrahedron. These tetrahedra are joined by the sharing of oxygen ions at three of the four corners into a hexagonal net having the composition $(AlSi_3O_{10})_n$ with the unshared oxygen ions coplanar as shown in Fig. 1c. Two such sheets are combined by octahedral coordination about aluminum, magnesium, iron, etc., of the unshared oxygen ions and of hydroxyl ions at the centers of the plane hexagons formed by the oxygen ions. A layer of this type having the composition $[Mg_3AlSi_3O_{10}(OH, F)_2]^-$ is shown in projection in Fig. 1a, and a similar one for muscovite $[Al_2AlSi_3O_{10}(OH, F)_2]^-$ is illustrated in Fig. 1b. The complete structure is formed by joining such layers with potassium ions at the centers of the hexagons in the projection of Fig. 1a and 1b, each of these potassiums having twelve neighboring oxygen ions, six being in the top of one layer and six in the bottom of another. The perfect cleavage, characteristic of the micas, is between the layers.

---

* Pauling indicated in a conversation with Foshag and Hendricks about five years ago that he suspected polymorphism among the micas.

[1] *Proc. Nat. Acad. Sci.*, **16**, 123 (1930).

[2] *C. R.*, **185**, 228 (1927); **186**, 879 and 1131 (1928).

[3] *Zeits. Krist.*, **76**, 211 (1930); **85**, 160 (1933).
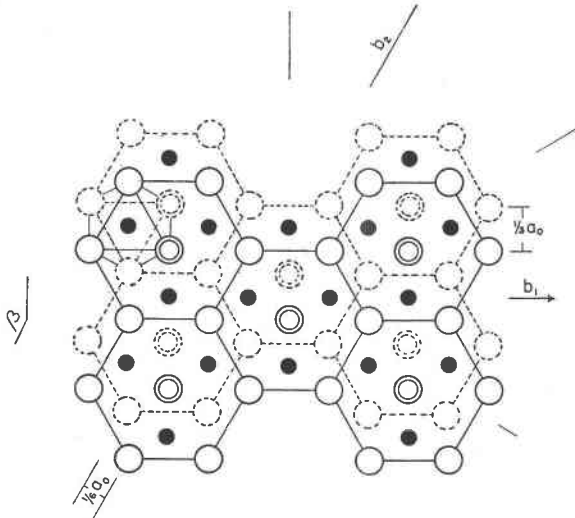
FIG. 1a. Projection on (001) of a portion of a phlogopite layer, $Mg_3AlSi_3O_{10}(OH,F)_2K$. In all the figures illustrating structure small black circles represent ions having octahedral coordination, in the plane of the projection: Mg, Li, Al, Fe, etc. Oxygen ions and hydroxyl groups 1.1Å from the plane of projection are shown as large circles; solid above, and dotted below. The hexagons are schematic representations of the atomic grouping of Fig. 1c. Potassium ions 5.0Å from the plane of projection are shown by small open circles. The b axis has the orientation b_1 in the single layer structure.
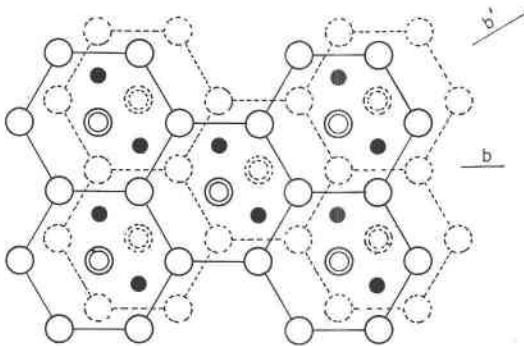

FIG. 1b. Projection on (001) of a portion of a muscovite layer $Al_2AlSi_3O_{10}(OH,F)_2K$.
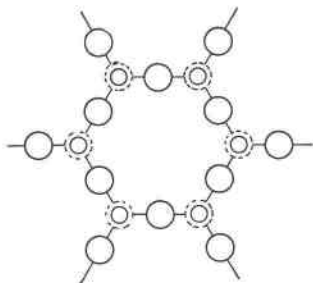
FIG. 1c. A projection of a hexagonal ring of SiO_4 tetrahedra joined by the sharing of oxygen ions. Dotted circles represent oxygen ions at the tetrahedra apexes, 2.2Å below the plane of projection in which the remaining oxygen ions are situated. Silicon ions 0.60Å below the projection planes are shown as small circles.
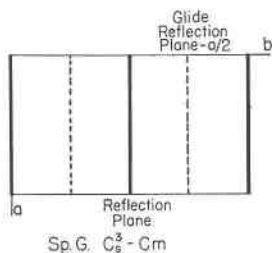

Sp. G. C_s^3 - Cm

FIG. 1d. Symmetry elements of the space group $C_s^3 - m$ for the single layer structure. The layer has these symmetry operations.

Muscovite crystallizes in the monoclinic system and the $[[Al_2]$ $(AlSi_3)O_{10}(OH, F)_2]_n^{n-}$ layers are related as shown in Fig. 1b to the unique monoclinic axis b. The unit of structure of muscovite according to the measurements of Jackson and West has the constants

$$a_0 = 5.18\text{Å} \qquad c_0 = 20.04\text{Å} \qquad \text{Space group } C_{2h}^6 - C2/c$$
$$b_0 = 9.02\text{Å} \qquad \beta = 95°30'$$

with $2[Al_2(AlSi_3)O_{10}(OH, F)_2K]_2$ in the unit of structure. Two layers are related by the glide reflection planes, n and c, of the space group. (Note Fig. 3b.) The monoclinic angle β is determined by these symmetry elements and the requirement that potassium ions between layers have twelve-fold coordination with respect to neighboring oxygen ions; $c_0 \cos \beta$ being about equal to $\frac{1}{3}a_0$.

Mauguin states that the biotite and phlogopite units of structure have the constants

Biotite	$a_0 = 5.30\text{Å}$	$c_0 = 10.16\text{Å}$
	$b_0 = 9.21\text{Å}$	$\beta = 99°3'$
Phlogopite	$a_0 = 5.32\text{Å}$	$c_0 = 10.24\text{Å}$
	$b_0 = 9.21\text{Å}$	$\beta = 100°2'$

Descriptions of the mica structure are also given by W. L. Bragg[4] and by R. E. Stevens[5] in a paper that appeared recently in this journal.

Naming of the various micas is a difficult question, especially in the absence of complete chemical analyses. In the following work the mineral name as indicated on the specimen is given, and is probably trustworthy. The name biotite used in the structure discussion is often synonymous with octophyllite, a term originated by A. N. Winchell.[6]

Experimental Procedure

Crystals elongated parallel to various directions in the cleavage plane were cut to a size suitable for x-ray work, from cleavage sheets of the micas. These were usually cut parallel to the extinction directions if the sheets had observable birefringence in the cleavage plane. If the mica was very darkly colored, or practically uniaxial, the orientation was determined from Laue photographs. Crystals were cut with elongations parallel and perpendicular to the b- or pseudo b-axes. Some distortion was unavoidable and for this reason fragments were not always reduced to sufficiently small dimensions to avoid considerable absorption of x-rays. Some of the samples contained crystals less than .2 mm. in their maximum dimension and these were examined without cutting. Large folia were studied in several cases in order to eliminate any question of distortion.

Weissenberg x-ray goniometer equatorial zone photographs were taken for all the crystals with rotation about the a- or pseudo a-axes. In the majority of the cases equatorial zone photographs were also taken with rotation about the b- or pseudo b-axes, and rotating crystal photographs were taken about the a- and b- or pseudo a- and b-axes. Laue photographs were obtained from about twenty-five specimens.

Photographs of the above type as well as 1st layer line Weissenberg goniometer photographs with rotation about the a- and b- or pseudo a- and b-axes, and the 3rd layer line about the b- or pseudo b-axes were made in every case from at least two different specimens showing the structures examined in detail.

Cu K radiation was used throughout even though some of the micas contained large amounts of iron. Intensities of reflections were visually estimated and the accuracy obtained is adequate for this work. Atomic F values listed in the "International Tables for the Determination of Crystal Structures" (I.T.D.C.S.) were used in all intensity calculations. The Lorentz and polarization factors were taken into account, the factor

[4] *Atomic Structure of Minerals*, Cornell Univ. Press, Ithaca, N. Y., **1937**.

[5] *Am. Mineral.*, **23**, 607 (1938).

[6] *Am. Jour. Sci.* (V), **9**, 309 and 415 (1925).

depending upon the angle of diffraction being $\dfrac{1 + \cos^2 2\theta}{\sin 2\theta}$. All calculated intensities listed are divided by 160 and are reduced by the necessary volume factor to make them comparable to that given for the single layer monoclinic unit of structure. Atomic coordinates are those listed in I.T.D.C.S.

Accurate measurements of crystal constants were outside the scope of this work. However, it was qualitatively observed that the values did not differ appreciably from those previously found except, of course, that there were various choices of β or its pseudo value. When β is given as 90° for a particular structure it is to be understood that the value is accurate to within $\pm 30'$.

The Single Layer Structure of the Micas
(monoclinic hemihedral)

Biotite samples Nos. 78303 and 48309, phlogopite C3644, and lepidolite 93924 (analyzed) were thoroughly examined. Lattice dimensions of the phlogopite and biotite specimens were the same within the limits of error as those found by Mauguin, which requires $c_0 \sin \beta$ to be 10.0Å. The unit of structure therefore contains a portion of a single layer; which for phlogopite is $2[Mg_3AlSi_3O_{10}(OH, F)_2K]$, for biotite $2[(Mg, Fe, Al)_3-AlSi_3O_{.0}(OH, F)_2K]$ and for polylithionite $2[Li_2AlSi_4O_{10}F_2K]$ (which lepidolite 93924 approximates in composition).

The net of lattice points normal to the b-axis is shown in Fig. 2, and $ABCD$ is the projection of the unit cell selected. This, of course, is arbitrary, $GIJH$ etc. being equally satisfactory. More complex cells such as $GKLH$ crossing two layers, and $AEFD$ crossing three layers can be selected. The latter has the monoclinic angle β equal to 90°, the translation Bf being just one-third of a_0, BC. Rotating crystal photographs taken about AB, AE, and GK as axes of rotation give layer line periodicities 1×10Å, 3×10Å, and 2×10Å, respectively.

There is only one way in which the simplest unit of structure can contain a portion of one mica layer. Atomic coordinates of this arrangement having the orientation b_1, of Fig. 1a are given in Table I. The structure is isomorphous with the monoclinic hemihedral point group $C_s - m$, the space group being $C_s{}^3 - Cm$.

Relative intensities of various $(h0l)$, $(0kl)$, $(19l)$, and $(11l)$ reflections calculated for phlogopite, according to this structure, are listed in Tables II and III. All single layer mica samples have the same relative intensities of $(0kl)$, $k \neq n \times 3$, reflections, since the Al, Li, Mg, Fe, etc. atoms with octahedral coordination do not contribute to these reflections. A Weissenberg equatorial zone rotating about the a-axis is reproduced as Fig. 4a.
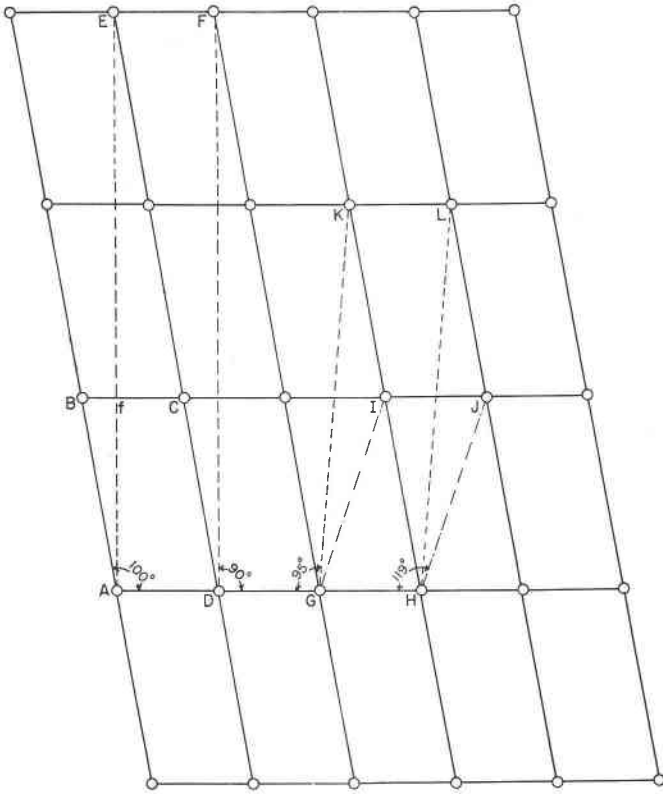
FIG. 2. Net of lattice points in (010) of the single layer monoclinic structure.

TABLE I

Atomic Coordinates for the Single Layer Structure. Space Group $C_s^3 - Cm$, $\beta = 100°$.

General Positions				Special Positions			
	x	y	z		x	y	z
4 O	.25	.25	.00	2 O	.00	.50	.00
4Si	.02	.33	.06				
4 O	.08	.33	.22	2(OH)	.08	.00	.22
4Mg	.44	.33	.34	2Mg	.44	.00	.34
4 O	.32	.17	.46	2(OH)	.32	.50	.46
4Si	.37	.17	.62				
4 O	.14	.25	.68	2 O	.39	.00	.68
				2K	.45	.50	.84

Table II

Approximate Observed and Calculated Intensities of Some $(h0l)$ Reflections of the Single Layer Phlogopite Structure, $Mg_3AlSi_3O_{10}(OH, F)_2K$.

l \ h	0		2^2		4		6		$\bar{2}$		$\bar{4}$		$\bar{6}$	
0			vs	170	a	2	vw	1						
1	ms[1]	80	vs	240	m-ms	50	vw	2	ms	70	ms	70	vw	1
2	w	9	s	130	vw	5	m	30	mw	5	s	90	ms	80
3	vs	250	mw	20	w	7			m	20	ms	40	mw	14
4	mw	7	s	170	ms	130			ms	70	vw	1	vw	4
5	vs	110	w	1	m	30			w	4	m	30	vw	2
6	m	60	mw	16					ms-s	150	s	90	m	30
7	m-ms	40	vw	2					ms	90	a	1	m	30
8	m-ms	50	m	30					vw	2	a	1	a	0
9	vw	2	vw	1					vw	2	a	1		
10	mw	15							m-ms	50				

[1] The following abbreviations are used in all tables: s, strong; m, medium; w, weak; vw, very weak.

[2] Observed intensities of $(20l_a)$ and $(13\,l_{a+1})$ are closely the same. Calculated values differ only in a small contribution due to oxygen.

* Reflections above the line arise from diffraction by transmission, those below from diffraction by reflection, from a highly absorbing crystal (several tenths of a mm. in thickness). Reflections such as $(20\bar{7})$ are affected by absorbtion. Similar conditions hold in other tables.

A striking regularity of the diffraction photographs is the pseudo-hexagonal character of the reflections for which the k index is a multiple of three, such as $(20l_a)$ and $(13l_{a+1})$. These planes are closely similar for the single layer structure as can be seen by referring them to the cell $AEFD$ of Fig. 2, which crosses three layers. The index transformations are as follows, the subscripts denoting layer multiplicity:

$$h_3 = h_1;\; k_3 = k_1;\; l_3 = 3l_1 + h$$

(201) becomes $(205)_3$ and $(13\bar{2})$ transforms to $(13\bar{5})_3$, which are equivalent hexagonal planes referred to orthohexagonal axes.

Intensity differences for some (hkl), $k = n \times 3$ reflections resulting from replacement of Mg in phlogopite by Li and Al, leading to lepidolite or polylithionite are shown in Table IV. Similar effects are observed and calculated for replacement of Mg by Fe, leading to biotite, annite, etc.

TABLE III

Approximate Observed and Calculated Intensities of Some Reflections of the Single Layer Phlogopite Structure, $Mg_3AlSi_3O_{10}(OH, F)_2K$.

l	(02l)		(04l)		(06l)		(19l)[1]		(19$\bar{l}$)[1]		(11$\bar{l}$)	
0	ms-m	60	m	40	vs	200	w	8			mw	15
1	w	2	m	40	mw	20	a	1	w	8	mw-w	11
2	s	120	mw	20	vw	1	mw	20	m	25	ms-s	90
3	ms	90	w	2	w	2	mw	16	w	7	s	130
4	vw	1	mw-w	5	mw	25	a	1	a	1	w	11
5	vw	2	vw	1	mw-w	15	m	50	m	30	vw	2
6	mw-w	4	mw	30	vw	2	m	50				
7	mw	12	mw	30	m-mw	35						
8	vw	1	vw	1	m-mw	30						
9	vw	0	mw-w	7								
10	w	2	vw	1								

[1] Structure factors of (19l) and (13l) reflections are equal. Differences in intensities are a result of different polarization and Lorentz factors and change of F values with $\sin \theta / \lambda$

TABLE IV

Approximate Observed and Calculated Intensities of Some Reflections of Phlogopite and Lepidolite.

Plane[1]	Phlogopite 4463		Lepidolite 86193	
203	mw	20	vw	3
20$\bar{3}$	mw	20	vw	2
20$\bar{4}$	ms	70	m	20
20$\bar{5}$	w	4	m	20
20$\bar{8}$	vw	2	vw	2
400	a	2	vw	3
40$\bar{5}$	m	30	w	15
062	vw	1	a	0

[1] (0kl), $k \neq n \times 3$, intensities are not influenced by substitution in the octahedral positions, i.e., Mg, Al, Fe, etc., by Li. Other ($h0l$) intensities show smaller variations, these listed being among the more pronounced ones.

THE TWO LAYER STRUCTURE OF THE MICAS; MUSCOVITES, BIOTITES, ETC. (MONOCLINIC HOLOHEDRAL)

Phlogopite sample 78218, biotite P. R. C. 395, and a commercial muscovite sample were thoroughly examined. The only possible two layer structure preserving the usual mica layer and twelve-fold coordination of potassium is that shown in Fig. 3a. It is isomorphous with point group $C2_h - 2/m$ and is derived from space group $C_{2h}{}^6 - C2/c$ (Fig. 3b) by choice of an appropriate value of β corresponding to cell GKLH of Fig. 2. This is the structure found for muscovites by Jackson and West and their parameter values are listed in Table V.

TABLE V

Atomic Coordinates for the Two Layer Structure, $\beta = 95°$. Space Group $C_{2h}{}^6 - C2/c$.

General Positions				Special Positions			
	x	y	z		x	y	z
8Mg	.25	.083	.000	4Mg(d)	.75	.25	.000
8Si	−.033	−.250	.135	4K(e)	.00	.083	.250
8Si	−.033	.417	.135				
8 O	.228	.333	.164				
8 O	.228	−.167	.164				
8 O	.480	.083	.164				
8 O	−.062	−.167	.055				
8 O	−.062	.417	.055				
8 (OH)	−.062	.083	.058				

Intensities of (h0l) reflections for the two layer phlogopite structure are the same as those given for the single layer structure in Table II after the necessary index transformation. Calculated and observed intensities of some (0kl) reflections for muscovite are listed in Table VII together with the structure amplitudes calculated by Jackson and West. A most important factor appears, namely (06l) reflections with l odd are observed and this is true for all the muscovite samples. Such reflections are required to be absent by the ideal structure and can only be explained by considerable departure from the structure given by Jackson and West. They are absent for the two layer biotite-like micas and none is observed for any of the micas that give the (h0l) intensities of the single layer structure (except muscovite). These characteristics are illustrated by the photographs reproduced as Figs. 4a and 4d.

TABLE VI

Approximate Observed and Calculated Intensities of Some (0kl) Reflections of the Two Layer Phlogopite Structure.

$k\rightarrow$ $l\downarrow$	2		4		6		8	
0	w	$\bar{3}$	w	30	vs	200	a	2
1	m	40	mw—w	15	a	0	a	0
2	vw	2	w—	5	mw	20	a	0
3	s	120	w+	10	a	0	w—	10
4	m	50	w—	10	vw	1	vvw	3
5	ms	70	vw	5	a	0	vw	5
6	mw	25	vw	3	w	2	a	0
7	w	10	w	12	a	0		
8	a	0	vw	5	m	25		
9	a	2	a	0	a	0		
10	a	0	a	5	mw	15		
11	a	0	w	20	a	0		
12	a	2	vw	5	a	2		
13	w	15	w	20	a	0		
14	vw	3	vw	5	mw	35		
15	vw	3	vw	3	a	0		
16	a	0	a	0	m	30		
17	a	0	w—	5	a	0		

TABLE VII

Calculated Structure Amplitudes for Muscovite After Jackson and West. Observed Intensities for Cu K Radiation.

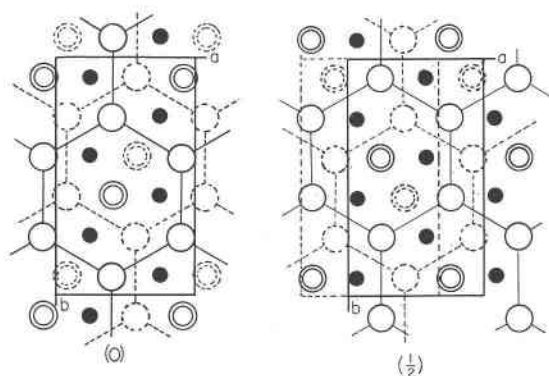| $k\rightarrow$ $l\downarrow$	2		4		6	
0	w	4	w	18	vs	65
1	w	11	mw	18	w	0
2	mw	8	m		w+	16
3	m	21	mw	16	a	0
4	m+	24	m	14	a	1
5	ms	35	a	4	vw	0
6	a	7	w	9	w	4
7	w		vw		vw	0
8	a		a	0	m	26
9	a		a		w	
10	vw		vw		w	

Fig. 3a. Sequence of layers in the two layer monoclinic holohedral structure.
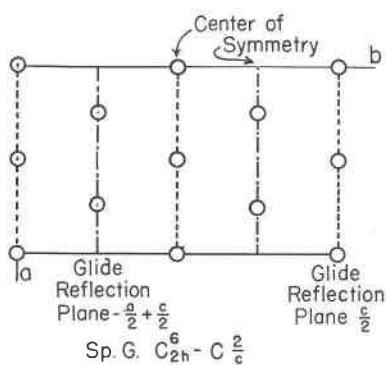

Fig. 3b. Symmetry elements of the space group.

Muscovite then has a distinctly different structure from the two layer biotites. It would be difficult to determine the exact departure from the ideal and for this reason a close analysis has not been made at this time. The coordinates given in Table V are accurate for the two layer biotite type structure.

Calculated intensities for $(0kl)$ reflections listed in Table VI are very sensitive to choice of atomic scattering powers, particularly for oxygen. Several poor agreements in the table are explained in this manner. The poorest is (040), the calculated intensity of which is too high compared with the neighboring (041) and (043) reflections. The high calculated value of (04.10) is due entirely to a pronounced oxygen contribution which a thermal factor would greatly decrease. Similar effects appear in the various tables for the other micas.

Fɪɢ. 4. Weissenberg equatorial zone photographs of various micas with crystals rotating about a- or pseudo a-axes (except 4h), Cu K radiation.

Reflection
Plane
m

00ℓ

06ℓ →
04ℓ →
02ℓ →

←Trace
of
crystal
distortion

Trace of
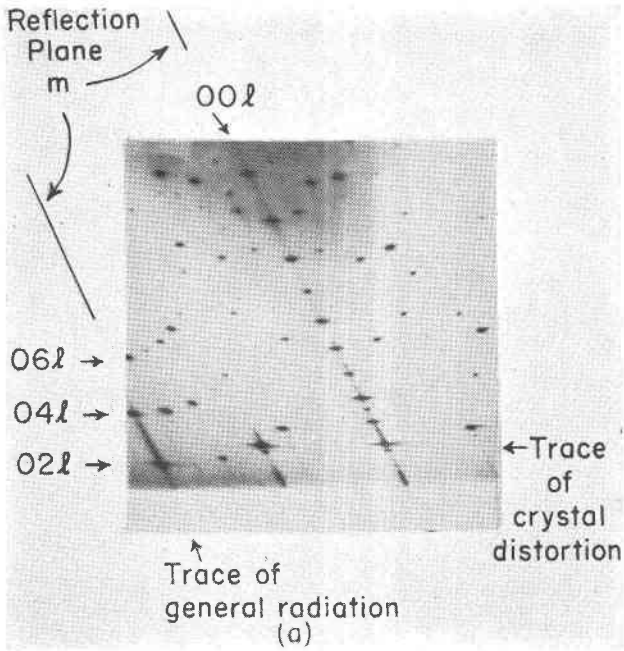general radiation
(a)

Fɪɢ. 4a. Single layer monoclinic hemihedral phlogopite that does not show diffuse scattering.
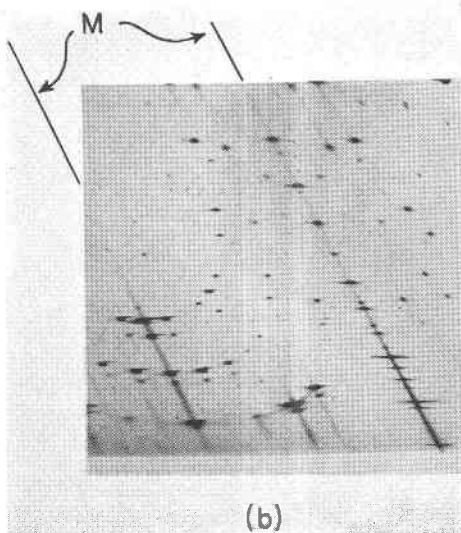
M

(b)

Fɪɢ. 4b. Single layer monoclinic hemihedral phlogopite with weak diffuse scattering.
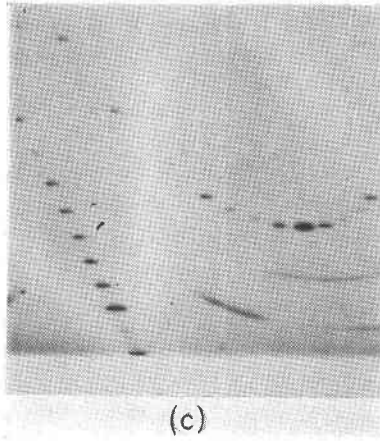
Fɪɢ. 4c. Single layer monoclinic hemihedral biotite with very diffuse scattering.
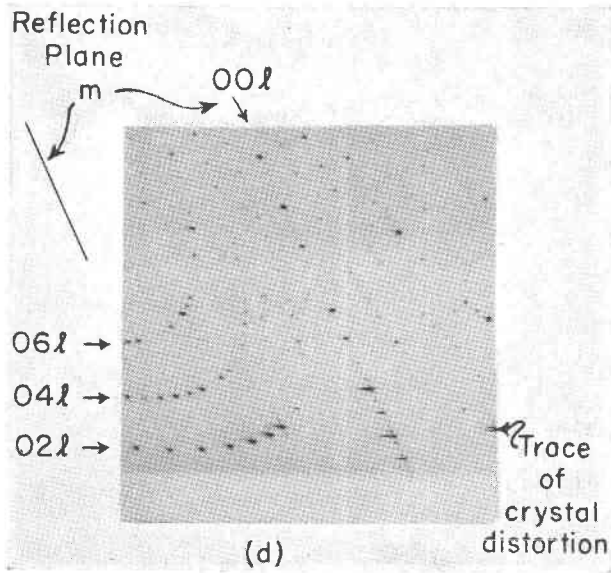
Fɪɢ. 4d. Muscovite, two layer monoclinic holohedral.
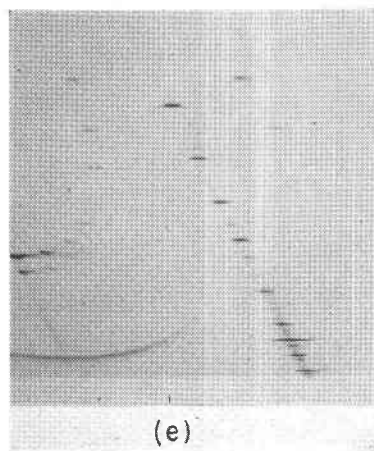
FIG. 4e. Two layer monoclinic holohedral biotite with very diffuse scattering.

FIG. 4f. Three layer rhombohedral enantiomorphic hemihedral phlogopite, weakly developed diffuse scattering.

FIG. 4g. Six layer monoclinic hemihedral lepidolite (compare with 4h).

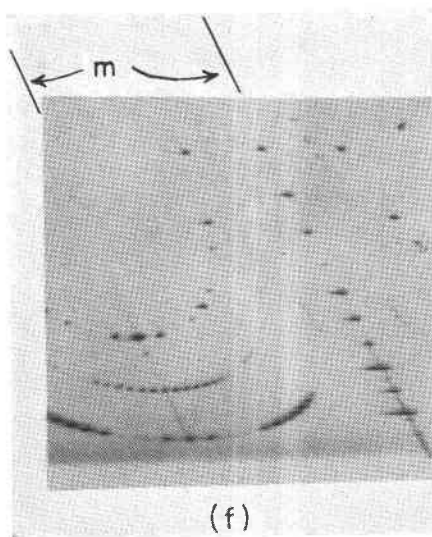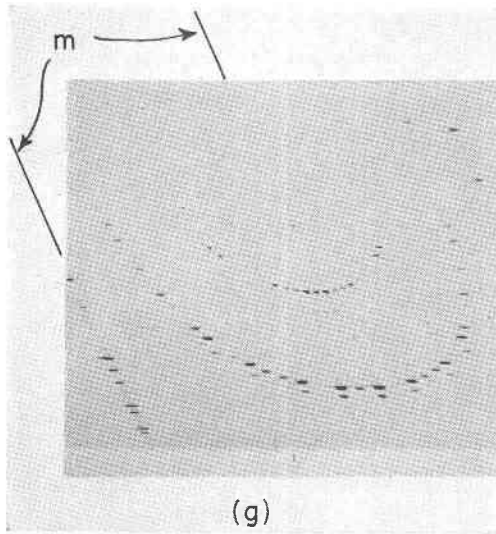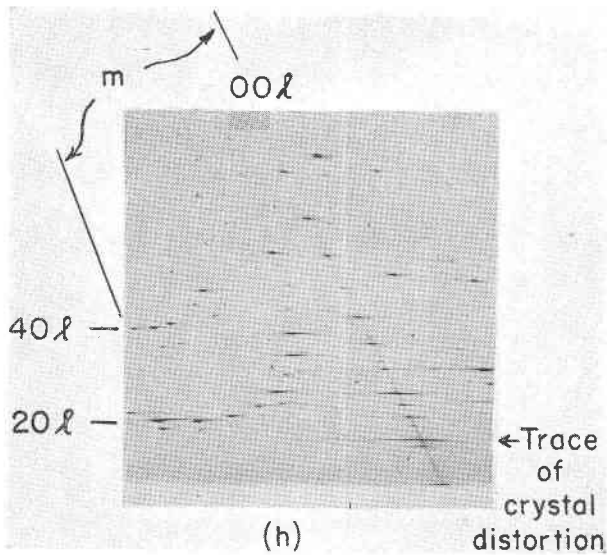FIG. 4h. Single layer monoclinic hemihedral phlogopite with
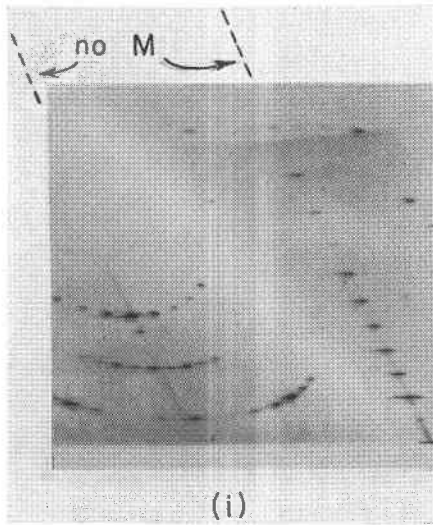crystal rotating about b-axis.

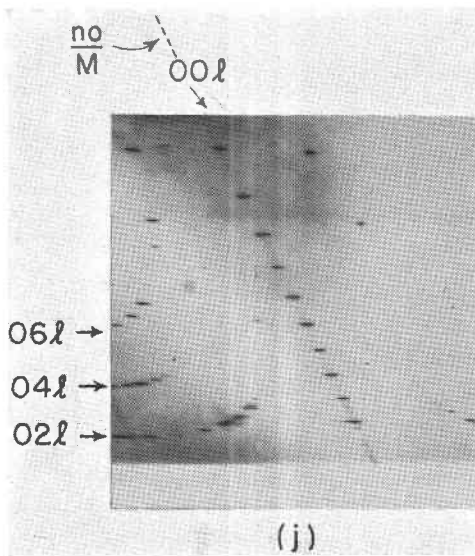FIG. 4i. Six layer triclinic holohedral biotite. Note absence of reflection planes.

FIG. 4j. Twenty-four layer triclinic holohedral biotite.

THE THREE LAYER STRUCTURE (RHOMBOHEDRAL ENANTIO-
MORPHIC HEMIHEDRAL. LOW-QUARTZ CLASS)

Phlogopite sample No. 4463 and lepidolite No. R4365 (analyzed) were carefully examined. All crystals of this type are closely uniaxial and Laue photographs with the x-ray beam normal to the cleavage appear to have a three-fold axis and three planes of symmetry (D_{3d}). Indices can be assigned to all reflections by use of a hexagonal unit of structure having $a_0 = a$ (single layer monoclinic structure) $= 5.3$Å, for phlogopite and $c_0 = 3 \times c$ (single layer monoclinic structure). Moreover $(2\overline{1} \cdot l_a)_{\mathrm{Hex}}$ reflections have the same intensities as the $(h0l_a)_1$ reflections.

With the above limitations it is necessary to find a hexagonal or pseudo-hexagonal three layer structure having the same projection on (01.0) as does the single layer structure on $(010)_1$. This can only be done in two ways and these are enantiomorphic. Atomic coordinates of the resulting structure illustrated in Fig. 5b are listed in Table VIII. A particular layer is repeated about a three-fold screw axis normal to the cleavage. The space group is $D_3{}^3 - C3_1 12$ or $D_3{}^5 - C3_2 12$. (Fig. 5a).

Agreement between observed and calculated intensities is shown in Tables IX and II (after index transformation). Presence of lithium in the lepidolites modifies the intensities as shown by Table IV and as was discussed for the single layer structure; a Weissenberg goniometer photograph with rotation about the orthohexagonal b-axis is reproduced as Fig. 4f and a Laue photograph taken with the x-ray beam approximately normal to (00.1) is shown in Fig. 9c.

TABLE VIII

Atomic Coordinates for the Three Layer Structure. Space Group $D_3{}^3 - C3_1 12$.
Rhombohedral Enantiomorphic Hemihedral.

	General Positions				Special Positions	
	x	y	z		x	z
6Si	$-.22$	.22	.078	3K	.11(1/9)	.000(0)
6Si	.44	$-.44$	.078	3Mg	.11(1/9)	.167(1/6)
6 O	.11	.39	.060	3Mg	$-.22(2/9)$	.167(1/6)
6 O	$-.39$	$-.11$	.060	3Mg	.44(4/9)	.167(1/6)
6 O	$-.39$	.3)	.060			
6 O	$-.22$	.22	.130			
6 O	.44	$-.44$	.130			
6(OH)	.11	$-.11$	.130			

TABLE IX

Approximate Observed and Calculated Intensities of Some (0kl) Reflections of the Three Layer Rhombohedral Enantiomorphic Hemihedral Phlogopite Structure.

$k \rightarrow$ $l \downarrow$	1		2		3		4
0	w	15	mw	20	vs	200	a
1	mw	20	mw	45	a	0	a
2	a	2	mw	20	a	0	vw
3	vw	5	mw	20	mw	20	a
4	m	30	mw	25	a	0	vw
5	ms	160	vw	5	a	0	vvw
6	s	200	w	7	a	1	vvw
7	ms	130	a	0	a	0	vvw
8	m	80	a	1	a	0	
9	mw	35	w	10	a	2	
10	w	20	vw	1	a	0	
11	vw	10	w	10	a	0	
12	a	0	vw	5	m	25	
13	a		vw		a	0	
14	a		a		a	0	
15	a		a		mw	15	

THE SIX LAYER LEPIDOLITE STRUCTURE
(MONOCLINIC HEMIHEDRAL)

Lepidolite samples No. 97893 and Stevens No. 6, both of which were analyzed specimens, were carefully examined. Laue photographs taken with the x-ray beam normal to the cleavage although badly distorted show only a plane of symmetry. The crystals therefore must be monoclinic. Weissenberg equatorial zone photographs taken with crystals rotating about axes parallel to the extinction directions in the cleavage plane show that the b-axis is 5.3Å and the a-axis 9.2Å, which are interchanged in comparison with the other monoclinic micas. Moreover these lepidolites gave (0kl) reflections entirely different from the analogous (h0l) reflections of other micas examined as can perhaps be seen from the photographs reproduced in Figs. 4g and h. The monoclinic angle β can be taken as 90°.

The c-periodicity is six times c_0 of the single layer structure, therefore the unit of structure is crossed by six mica layers. Reflections so far as tested were present only from planes having $\dfrac{3k-h}{2}+1=3n$, which is the rhombohedral requirement for orthohexagonal indices. Reflections are absent from (h0l) with l odd, but are present from (11l) with l odd.

These conditions are strictly the same as were found for the kaolin mineral nacrite[7] which is monoclinic, the space group being C_s^4-Cc, but closely approaches the requirements of the rhombohedral space group C_{3v}^6-R3c. However while a kaolin layer in which positions with octahedral coordination are completely filled has a three-fold axis, the mica layer can not have this symmetry as perhaps can be seen from the various figures.

In order to determine the structure it is necessary to combine six mica layers according to the symmetry operations of space group $C_{3v}-Cc$ and still have the types of absent reflections indicated above. If there is a pseudo space group it cannot be rhombohedral since all rhombohedral groups have three-fold axes. The only groups that can be used are those having only three-fold screw axes, namely $C_3^2-C3_1$ and $C_3^3-C3_2$ (Fig. 6b). These combined with C_s^4-Cc (Fig. 6a) lead to the necessary structure.

This procedure is very interesting since it combines a three-fold screw axis with a glide reflection plane which converts it into a screw axis of opposite sense. The operations of such a group are not closed so that it is not one of the possible space groups. However it leads to a simpler description of the crystal than does the ordinary space group C_s^4-Cc. In short the symmetry operations of the crystal can be considered as right and left three-fold screw axes, with an *arbitrary origin*, repeated by a glide reflection of $c=\frac{1}{2}c_0$ about a plane including the axes.

Atomic coordinates referred to space group C_s^4-Cc are listed in Table X and it can be seen that 180 parameters are required to describe the structure. Agreement between observed and calculated intensities is shown in Tables XI and XII. The structure is illustrated in Fig. 6c.

[7] Hendricks, S. B., *Zeits. Krist.*, **100**, 509 (1939).

TABLE X

Atomic Coordinates of the Six Layer Pseudo-rhombohedral Monoclinic Lepidolite Structure. Space Group $C_s^4 - Cc$.

	1st layer			2nd layer			3rd layer		
	x	y	z	x	y	z	x	y	z
4K	.00	1/3	a[1]	1/3	2/3	1/6+a	1/6	5/6	1/3+a
4 O_1	1/4	1/12	b[1]	1/12	5/12	1/6+b	1/6	1/3	1/3+b
4 O_2	1/4	7/12	b	1/3	1/6	1/6+b	5/12	1/12	1/3+b
4 O_3	1/2	1/3	b	1/12	7/12	1/6+b	5/12	7/12	1/3+b
4Si_1	1/3	1/3	c[1]	0	2/3	1/6+c	0	1/3	1/3+c
4Si_2	1/6	5/6	c	1/6	1/6	1/6+c	1/3	1/3	1/3+c
4 O_4	1/3	1/3	d[1]	0	2/3	1/6+d	0	1/3	1/3+d
4 O_5	1/6	5/6	d	1/6	1/6	1/6+d	1/3	1/3	1/3+d
4OH_1	0	1/3	d	1/3	2/3	1/6+d	1/6	5/6	1/3+d
4Mg_1	0	0	e[1]	0	0	1/6+e	0	0	1/3+e
4Mg_2	1/6	1/2	e	1/6	1/2	1/6+e	1/6	1/2	1/3+e
4Mg_3	1/3	0	e	1/3	0	1/6+e	1/3	0	1/3+e
4OH_1'	1/6	1/6	f[1]	0	1/3	1/6+f	1/3	2/3	1/3+f
4 O_5'	0	2/3	f	1/6	5/6	1/6+f	0	2/3	1/3+f
4 O_4'	1/3	2/3	f	1/3	1/3	1/6+f	1/6	1/6	1/3+f
4Si_2'	0	2/3	g[1]	1/6	5/6	1/6+g	0	2/3	1/3+g
4Si_1'	1/3	2/3	g	1/3	1/3	1/6+g	1/6	1/6	1/3+g
4 O_3'	1/6	2/3	h[1]	0	5/6	1/6+h	1/12	5/12	1/3+h
4 O_2'	5/12	5/12	h	1/4	1/12	1/6+h	1/12	7/12	1/3+h
4 O_1'	5/12	7/12	h	1/4	7/12	1/6+h	1/3	1/6	1/3+h

[1] In this table $a = .0825$, $b = .053 = -h$, $c = .044 = -g$, $d = .017 = -f$, $e = .000$.

TABLE XI

Approximate Observed and Calculated Intensities of Some ($h0l$) Reflections for the Six Layer Pseudo-rhombohedral Monoclinic Lepidolite. Note that $a = 9.0$Å, $b = 5.3$Å.[1]

202	ms	30	40$\bar{2}$	m	20	600[2]	vs	200
208	s	60	40$\bar{8}$	mw	10	606	m	20
2014	vs	200	40$\overline{14}$	w	4	6012	a	0
2020	m	25	40$\overline{20}$	mw	10	6018	a	0
2026	a	1	40$\overline{26}$	a	3	6024	m	15
2032	a	0	40$\overline{32}$	mw	20	6030	mw	6
2038	mw	20	40$\overline{38}$	mw	15	6036	a	0
20$\bar{4}$	mw	10	404	ms	50			
20$\overline{10}$	vs	150	4010	s	90			
20$\overline{16}$	vs	150	4016	vw	6			
20$\overline{22}$	w	4	4022	mw	20			
20$\overline{28}$	vw	2	4028	a	2			
20$\overline{34}$	w	5	4034	m	30			

[1] Only planes with pseudo-rhombohedral indices are present.

[2] (60l) and (60$\bar{l}$) observed and calculated intensities are identical.

TABLE XII

Observed and Calculated Approximate Intensities of Some (0kl) Reflections of the Six Layer Pseudo-rhombohedral Monoclinic Lepidolite. Note that $a = 9.0$Å, $b = 5.3$Å.

$k \rightarrow$ $l \downarrow$	2		4		6	
0	mw	8	mw	15	vs	100
3	vs	100	ms	40	a	0
6	w	6	mw	8	a	0
9	s	60	mw	15	a	0
12	m	30	m	20	a	0
15	m	30	w	6	a	0
18	ms	50	a	2	a	0
21	w	5	a	0	a	0
24	a	1	a	0	w	3
27	ms	60	m	30	a	0
30	m	40	m	30	vw	2
33	a	0	vw	1	a	0
36	mw	30	vw	1		
39	mw	30	vw	1		
42	a	3	vw	1		

Sp. G. $D_3^3 - C3_1 12$
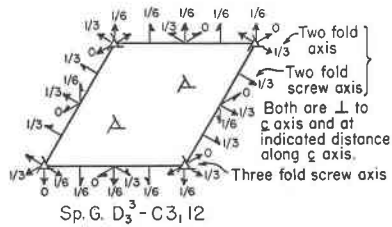
FIG. 5a. Symmetry elements of the space group.

$(\frac{1}{6})$ $(\frac{1}{2})$ $(\frac{5}{6})$
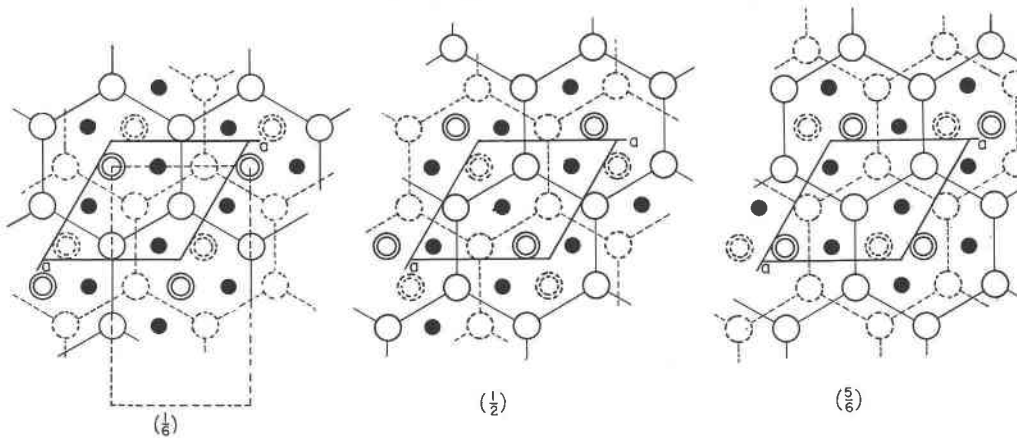
FIG. 5b. Sequence of layers in the rhombohedral enantiomorphic hemihedral structure.
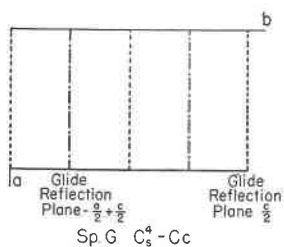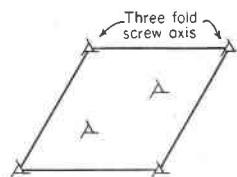
FIG. 6a. Symmetry elements of the space group.

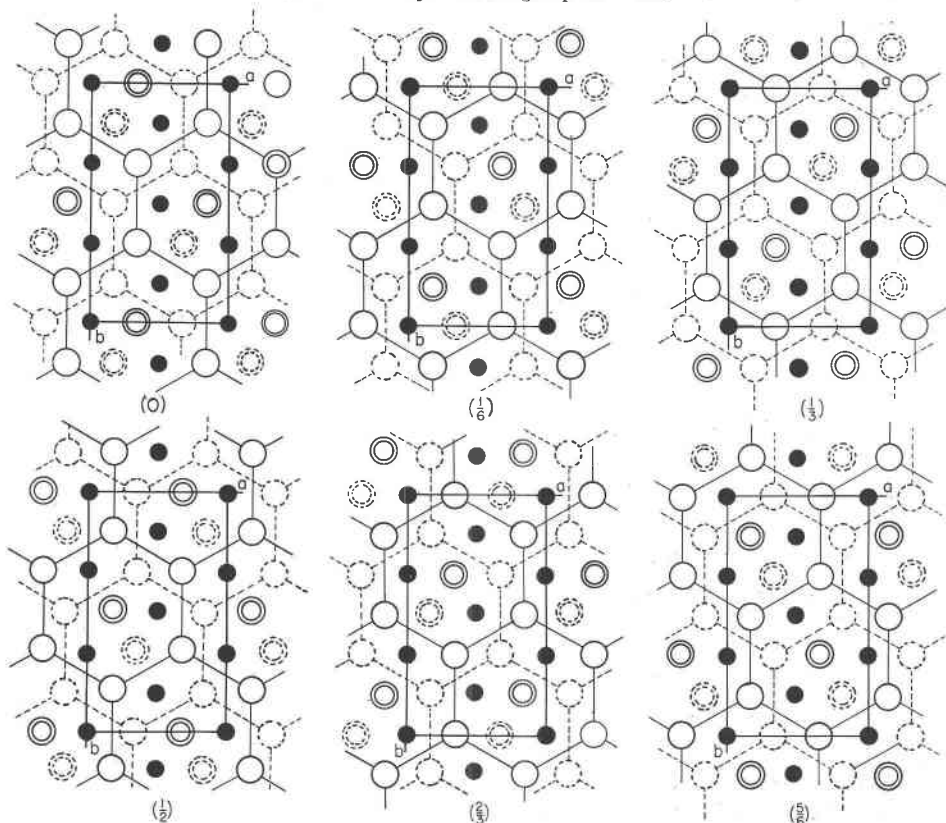FIG. 6b. The pseudo subgroup $C_3{}^2 - C3_1$.

FIG. 6c. Sequence of layers in the monoclinic hemihedral six layer structure. The layers as a whole are repeated by these symmetry operations.

THE SIX LAYER BIOTITE STRUCTURE
(TRICLINIC HOLOHEDRAL)

Biotite sample No. 3675 and one of the crystals from specimen No. 77436 were examined in detail. Laue photographs were too distorted for unambiguous determination of symmetry. The crystals were approximately uniaxial and Weissenberg equatorial zone photographs about the usual b- and pseudo b-axes were very similar. However neither these photographs nor ones taken about the a- and pseudo a-axes showed planes of symmetry normal to the cleavage.

A unit of structure can be selected that has the usual a- and b-dimensions of the one and two layer monoclinic micas. It has $c_0 = 6 \times c \sin \beta$ (single layer) and therefore is crossed by six layers. Moreover, reflections strictly analogous to the $(h0l)$ reflections of the single layer structure are observed with rotation about the pseudo b-axes. Assignment of indices to the various reflections according to this unit shows many types of general absences. Thus reflections are absent from $(0kl)$ (note Fig. $4i$) with $2k + l \neq 3n$, and $(11l)$ with $l \neq 2 + 3 \times n$ among others.

In the structure analysis it is necessary to explain the observed systematic absences by an atomic arrangement having the same projection on (010) as the single layer structure. Since these conditions are to be satisfied by all atoms, they must be satisfied by the potassium atoms. Without loss of generality the potassium positions must include one out of each of the following six sets:

	1(0)	2(1/6c)	3(1/3c)	4(1/2c)	5(2/3c)	6(5/6c)
a	000	1/3 0 1/6	1/6 1/6 1/3	0 1/2 1/2	1/3 0 2/3	1/6 1/6 5/6
b		1/3 1/3 1/6	1/6 1/2 1/3	0 1/3 1/2	1/3 1/3 2/3	1/6 1/2 5/6
c		1/3 2/3 1/6	1/6 5/6 1/3	0 2/3 1/2	1/3 2/3 2/3	1/6 5/6 5/6

and $x + \frac{1}{2}$, $y + \frac{1}{2}$, z. There are $3^5 = 243$ possible combinations.

The condition that the general absences be explained is fulfilled only by combination 1, 2a, 3a, 4c, 5b, 6c, i.e., with potassium at 000, 1/3 0 1/6, 1/6 1/6 1/3, 0 2/3 1/2, 1/3 1/3 2/3, 1/6 5/6 5/6 and these values repeated at $x + \frac{1}{2}$, $y + \frac{1}{2}$, z. The structure is completely determined by the added requirement of a mica layer and twelve-fold coordination of potassium with respect to oxygen.

The structure is isomorphous with the triclinic holohedral point group $C_i - \overline{1}$, the space group being $C_i^1 - P\overline{1}$. (Fig. 7b). One of the simplest units of structure has $a = b = 5.3$Å, $c = 6 \times 10$Å, $\beta = \alpha = 90°$, $\gamma = 120°$. It corresponds to the usual hexagonal cells. Atomic coordinates referred to these axes are listed in Table XIII and the structure is illustrated in Fig. 7a. Observed and calculated intensities are listed in Tables II (after index transformation) and XIV.

TABLE XIII

Atomic Coordinates of the Six Layer Triclinic Biotite Structure. Space Group $C_i^1 - P\bar{1}$.

	1st layer				2nd, 6th layer			3rd, 5th layer		
	x	y	z		x	y	z	x	y	z
4K	0	1/6	a[1]	4K	1/3	1/6	1/6+a	1/3	1/2	1/3+a
4Mg	1/3	1/6	e[1]	4Mg	0	5/6	1/6+e	0	1/6	1/2+e
2 Mg	0	1/2	e	4Mg	2/3	1/6	1/6+e	1/3	5/6	1/3+e
4 OH	0	1/6	d[1]	4Mg	1/3	1/2	1/6+d	2/3	1/2	1/3+d
4 O	1/3	5/6	d	4 OH	1/3	1/6	1/6+d	1/3	1/2	1/3+d
4 O	2/3	1/2	d	4 OH	0	1/6	1/6−d	1/3	1/6	1/3−d
4Si	1/3	5/6	c[1]	4 O	2/3	5/6	1/6+d	0	5/6	1/3+d
4Si	2/3	1/2	c	4 O	0	1/2	1/6+d	2/3	1/6	1/3+d
4 O	0	2/3	b	4 O	2/3	1/2	1/6−d	0	1/2	1/3−d
4 O	1/2	2/3	b	4 O	1/3	5/6	1/6−d	2/3	5/6	1/3−d
4 O	1/2	1/6	b							
4th layer				4Si	2/3	5/6	1/6+c	0	5/6	1/3+c
4Mg	1/3	1/6	1/2+e	4Si	0	1/2	1/6+c	2/3	1/6	1/3+c
2Mg	0	1/2	1/2+e	4Si	2/3	1/2	1/6−c	0	1/2	1/3−c
4 OH	2/3	1/2	1/2+d							
4 O	0	1/6	1/2+d	4Si	1/3	5/6	1/6−c	2/3	5/6	1/3−c
4 O	1/3	5/6	1/2+d	4 O	5/6	2/3	1/6+b	5/6	0	1/3+b
4Si	0	1/6	1/2+c	4 O	5/6	1/6	1/6+b	1/3	0	1/3+b
4Si	1/3	5/6	1/2+c	4 O	1/3	2/3	1/6+b	5/6	1/2	1/3+b
4 O	1/6	0	1/2+b	4 O	0	2/3	1/6−b	5/6	1/6	1/3−b
4 O	2/3	0	1/2+b	4 O	1/2	2/3	1/6−b	5/6	2/3	1/3−b
4 O	1/6	1/2	1/2+b	4 O	1/2	1/6	1/6−b	1/3	2/3	1/3−b

[1] In the table $a = .0825$, $b = .053$, $c = .044$, $d = .017$, $e = .000$.

TABLE XIV

Approximate Observed and Calculated Intensities of Some ($0kl$) Reflections of the Six Layer Triclinic Biotite Structure. Note that $a=b=5.3\text{Å}$, $\gamma=120°$, $\alpha=\beta=90°$.

$l\downarrow$	$k\rightarrow$ 1		2		4	
2	w	8	w	10	a	1
5	a	0	mw	30	vw	3
8	mw	12	w	8	vvw	1
11	ms	30	w	6	w	5
14	m	40	vw	1		
17	s	60	a	2		
20	w	6	vw	2		
23	vw	3	w	5		

$l\downarrow$	$k\rightarrow$ $\bar{1}$		2		$\bar{4}$	
1	mw	35	mw	35	a	1
4	vvw	1	w	10	a	1
7	w	20	mw	25	vw	3
10	m	35	w	3	vvw	2
13	s	150	w	3	vw	3
16	m	30	a	0		
19	m	25	vw	5		
22	vw	1	vw	2		
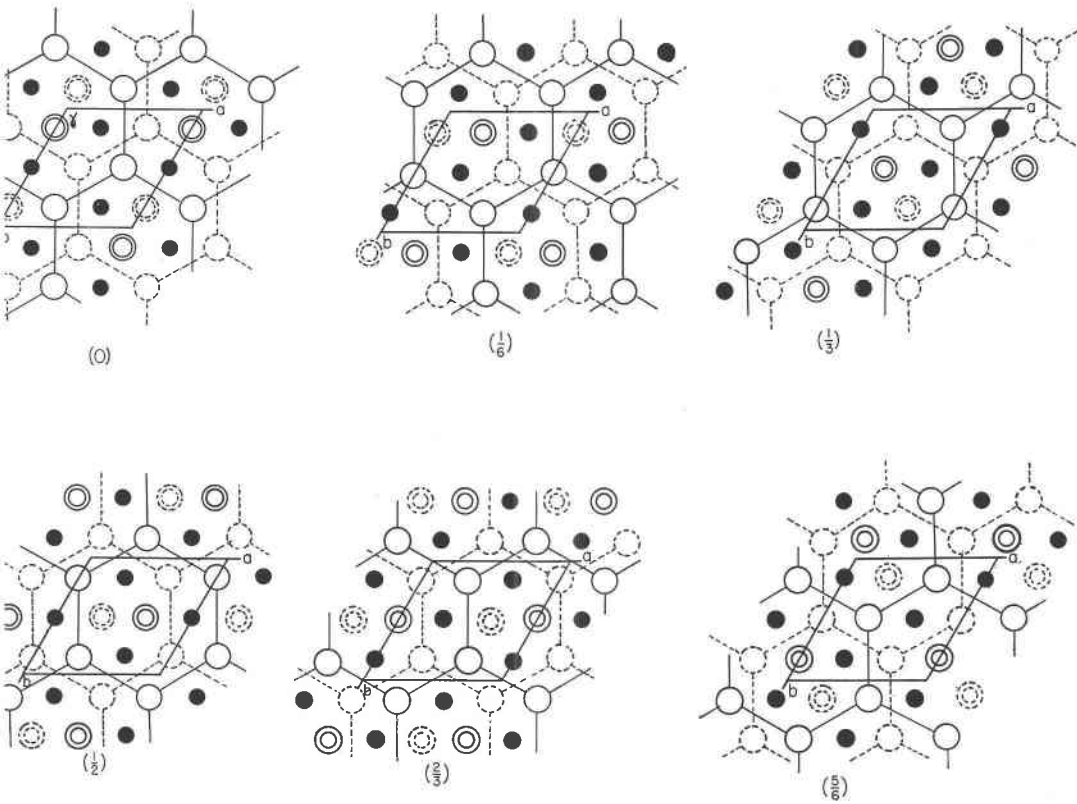
Fig. 7a. Sequence of layers in the six layer triclinic structure.
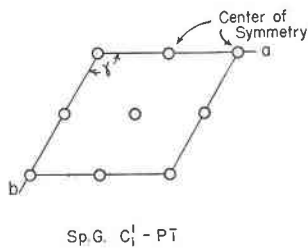

Sp. G. C_i^1 - P$\bar{1}$

Fig. 7b. Symmetry elements of the space group.

A Twenty-Four Layer Triclinic Structure

Sample No. 77436 from Ambulawa, Ceylon, contained a single mica crystal showing a very high layer periodicity. Photographs about the usual single layer pseudo *a*- and *b*-axes indicated that the symmetry is triclinic as also did Laue photographs one of which is reproduced as Fig. 9*d*. It is thus permissible to take the usual *a*- and *b*-directions as axes of the unit cell, the dimensions being $a = 5.3$Å, $b = 9.2$Å, $c = n \times 10$Å, $\gamma = 90°$, and $\beta = 90°$ with some question about α.

Reflections from (*hkl*) with $k = n \times 3$ are the same as were observed for the single layer structure. It is therefore necessary that the projection on (010) be the same as that of the single layer structure. A Weissenberg equatorial zone photograph with the crystal rotating about the triclinic *a*-axis is reproduced in Fig. 4*j*. It can perhaps be seen that the periodicity normal to the layer is very high and that an unambiguous index assignment would be difficult. After careful examination it was established that the (0*kl*) reflections closely reproduced the (0*kl*) reflections of the six layer triclinic structure as a partial group. Moreover the heavy trace of continuous scattering from (060) on an over-exposed photograph did not pass through any (02*l*) reflection but rather at a distance of about one-third the periodicity from the closest reflection.

TABLE XV

Observed Intensities of Some (0*kl*) Reflections of the Twenty-four Layer Triclinic Biotite and (in parentheses) the Six Layer Triclinic Structure $a = b = 5.3$Å, $\gamma = 120°$, $\alpha = \beta = 90°$.

l	*k* = 1	*l*	*k* = 1	*l*	*k* = 2	*l*	*k* = 2
2	vw	59	vw	76—(19)	w(w)	133	a
5	vw	62	a	79	a	136—(34)	w(w)
8—(2)	w(w)	65	vw	82	a	139	vvw
11	vw	68—(17)	ms(ms)	85	a	142	vvw
14	a	71	w	88—(22)	w(w)	145	vw
17	a	74	vw	91	vvw	148—(37)	w(vw)
20—(5)	a(a)	77	vw	94	vvw	151	a
23	a	80—(20)	w(w)	97	w	154	a
26	a	83	vvw	100—(25)	w(w)	157	a
29	vw	86	a	103	a	160—(40)	w(w)
32—(8)	m(mw)	89	a	106	a	163	vw
35	a	92—(23)	vw(vw)	109	a	166	vw
38	a			112—(28)	a(a)	169	w
41	a			115	a	172—(43)	w+(w+)
44—(11)	ms(ms)			118	a		
47	mw			121	vw		
50	w			124—(31)	w(w)		
53	w			127	a		
56—(14)	m(m)			130	a		

There are thus good reasons for supposing that the unit of structure is crossed by twenty-four mica layers. It is consistent with the above observations that the structure be triclinic holohedral with the cell dimensions

$$a=b=5.3\text{Å} \qquad c=24\times10\text{Å}$$
$$\alpha=\beta=90° \qquad \gamma=120°$$

similar to those of the six layer triclinic structure.

Observed intensities of some ($0kl$) reflections are listed in Table XV together with analogous ($0kl$) reflections of the six layer triclinic biotite. No attempt was made to complete the structure analysis although it does not appear impossible. There are 3^{23} combinations of twenty-four mica layers that will give the (010) projection.

OPTICAL PROPERTIES AND FREQUENCY OF OCCURRENCE OF VARIOUS STRUCTURES

Partial descriptions of the micas examined are listed under structure types in Tables XVI to XIX. It is realized that complete chemical analyses would have been desirable although they are not absolutely necessary. Many of the specimens were type materials from the Roebling collection of the U. S. National Museum. The lepidolite samples analyzed and described by R. E. Stevens[5] were available and are indicated under his numbers in the tables. Analyses also had been made of the taeniolite[8] sample, zinnwaldite from Amelia, Va.[9], alurgite from Cajon Pass, California[10] and muscovite from the Harding Mine, N. M..[11]

Some optical properties of the micas studied are listed in Tables XVI to XX. The maximum refractive index was measured either by immersion under the microscope, or by the Abbe total reflectometer when the Na$_D$ absorption was not too great. Only the latter method was used to obtain the minimum refractive index. The optic axial angle was measured by the Mallard method and is probably accurate to $\pm2°$ where a greater limit is not required by variability. It was thought that the refractive indices might be of some value as a rough measurement of the amount of iron present in the samples. The optic orientation was determined by examination of samples the crystallographic orientation of which had been determined by means of x-ray diffraction photographs.

[8] Miser, H. D., and Stevens, R. E., *Am. Mineral.*, **23**, 104 (1938).

[9] Glass, J. J., *Am. Mineral.*, **20**, 741 (1935).

[10] Webb, R. W., *Am. Mineral.*, **24**, 123 (1939).

[11] Analysis of Rocks and Minerals, *U. S. Geol. Survey, Bull.* **878**, 108 (1937).

TABLE XVI

Optical Properties and Numbers of Samples with the Single Layer Structure
(monoclinic hemihedral).

		α	γ	2V	Optic Orientation	Degree of Diffuseness
Biotites	U. S. N. M.					
78303	Wakefield, P. Q.	1.563	1.609	0°–5°		none
48309	Rossie, N. Y.	1.537	1.568	9°		none
48305	Pierrepont, N. Y.	1.54	1.59	8°–12°		VWD
R4454	Easton, Pa.	1.548	1.595	5°	‖ to (010)	WD
14459	Portland, Conn.	1.551	1.592	9°–10°	‖ to (010)	none
96204	Miask, Russia	1.566	1.618	6°–8°	‖ to (010)	VD
C3647	Succasunna, N. J.	1.557	1.612	6°–8°		VWD
82253	Grand Calumet Is., Can.		1.585	6°–8°	‖ to (010)	WD
P.R.C.1501	From a leucite monchiquite		1.61	0°–3°		none
P.R.C.266	From a nepheline syenite		1.63	3°–6°		WD
R4448	Anomite, Chester, Mass.		1.592	6°–9°	‖ to (010)	WD
R4449	Anomite, Greenwood Furnace, N. J.	1.560	1.604	5°–7°		MD
45960	Cryophyllite, Rockport, Mass.	1.545	1.57	20°–22°		none
R4472	Lepidomelane, Litchfield, Me.		1.64	3°		VD
Phlogopites						
C3644	Franklin, N. J.	1.530	1.558	7°		
13946	South Burgess, Ontario	1.543	1.582	8°–9°	‖ to (010)	none
86772	Franklin, N. J.		1.565	3°–5°	‖ to (010)	none
82023	Vroomans Lake, N. Y.	1.533	1.574	1°–3°	‖ to (010)	VD
78211	Somerville, N. Y.		1.565	5°–7°	‖ to (010)	none
92833	Pierrepont, N. Y.	1.544	1.582	0°		none
78216	Muscalunge Lake, N. Y.		1.575	5°–6°		VWD
103226	Magnet Cove, Ark.	1.590	1.613	0°–2°	‖ to (010)	none
R4468	Ogdensburg, N. J.	1.539	1.566	5°–6°	‖ to (010)	none
48300	DeKalb, N. Y.		1.575	5°–6°		none
82459	Burgess, Ontario	1.552	1.597	5°–7°	⊥ to (010)	WD
78214	Hammond, N. Y.		1.576	6°–8°	‖ to (010)	none
48278	Edwards, N. Y.		1.575	1°–2°		MD
Lepidolites, Polylithionites						
93924	Ramona, Calif., Stevens #15	1.533	1.555	45°	‖ to (010)	WD
86193	Haddam, Conn., with muscovite		1.56	48°–50°		none
84942	Mesa Grande, Calif.		1.562	50°		none
96239	Alaeschka, Russia		1.558	40°		MD
R4420	Haddam, Conn., with muscovite		1.558	35°–40°		none
R4425	Mt. Apatite, Me.		1.555	35°		none
94314	Kangerluar Suk, Greenland, Stevens #17		1.569	40°	‖ to (010)	none
Zinnwaldite						
86008	Zinnwald	1.539	1.564	30°	‖ to (010)	none
R4436	Brambach, Saxony		1.572	25°–35°	‖ to (010)	none
Samples from U. S. Geological Survey:						
Biotite	Magnet Cove (C. S. Ross) from nepheline pegmatite		1.625	10°–15°	‖ to (010)	none
Talniolite	Magnet Cove (W. T. Schaller)	1.523	1.553	0°		none
Phlogopite	Mendham, N. J. (Miss Glass)	1.538	1.570	5°–8°	‖ to (010)	MD

		α	γ	2V	Optic Orientation	Degree of Diffuseness
	U.S.N.M.					
Lepidolite	Stevens #8	1.56	30°–40°	‖ to (010)		
	Stevens #9	1.555	55°–58°	‖ to (010)	none	
	Stevens #10 U.S.N.M. 96012	1.562	30°	‖ to (010)	none	
	Stevens #13	1.558	25°–30°	‖ to (010)	none	
	Stevens #16	1.558	45°	‖ to (010)	none	
Zinnwaldite	Amelia, Va. (Miss Glass)					

TABLE XVII

Optical Properties and Numbers of Samples with the Muscovite Structure
(monoclinic holohedral).[1]

		α	γ	2V	Optic Orientation
Musco-vites	U.S.N.M.				
R4366	"Dutch East Africa"	1.570	1.615	37°–38°	⊥ to (010)
86193	Haddam Conn., with lepidolite		1.59	45°–47°	⊥ to (010)
89190	Pala, Calif.		1.578	43°–44°	⊥ to (010)
83775	Custer Co., S. D., with biotite	1.560	1.592	45°	⊥ to (010)
82021	Portland, Conn.	1.565	1.605	36°–38°	⊥ to (010)
46127	with biotite				
96460	Spruce Pine, N. C.	1.557	1.597	48°–50°	⊥ to (010)
C3677	with biotite				⊥ to (010)
C3648	Lincoln Co., N. C.	1.564	1.600	43°	⊥ to (010)
14349	Middleton, Conn., with biotite				
84430	Henry Co., Va.	1.563	1.605	38°–40°	⊥ to (010)
R4420	Haddam, Conn., with lepidolite	1.550	1.591	45°	⊥ to (010)
R4354	Catawaba Co., N. C.	1.556	1.605	34°	⊥ to (010)
96458	Oje Caliente, N. M.				
R7106	Mörefjar, Norway		1.61	42°	⊥ to (010)
Musco-vites	U. S. Geological Survey				
	Spruce Pine, N. C. (W. T. Schaller)	1.568	1.610	50°	⊥ to (010)
	Harding Mine, N. M. (W. T. Schaller)		1.59	47°–48°	⊥ to (010)
	Amelia, Va. (Miss Glass)	1.550	1.585	43°	⊥ to (010)
	North Carolina with biotite (C. S. Ross)	1.563	1.600	40°	⊥ to (010)
Lepidolite, Stevens #1			1.57	38°–40°	⊥ to (010)
Alurgite, Cajon Pass, Calif. (R. W. Webb)					

[1] None of the samples with the muscovite structure showed observable diffuse scattering in the $[h_a k_b l]$, $k_b \neq n \times 3$, zones.

TABLE XVIII

Optical Properties, Numbers, and Degree of Diffuseness of Samples with Various Multilayer Structures.

	α	γ	2V	Optic Orientation	Degree of Diffuseness
Two layer structure (monoclinic holohedral) U.S.N.M.					
Biotite P.R.C395, Montgomery Co., Ark.		1.625	10°–15°		none
Lepidomelane 7117, Brevig, Norway		opaque	ca 5°		none
Phlogopite 78218, Burgess, Ontario	1.54	1.57		$\perp$ to (010)	WD
Manganophyllite R4452, Pajsberg, Sweden		1.60	0°–2°		VD
Biotite 77436, Ambulawa, Ceylon					WD
Three layer structure (rhombohedral enantiomorphic hemihedral) U.S.N.M.					
Biotite, 93228, Torrington, New S. Wales		1.62	0°–3°		VD
C3677, with muscovite	1.585	1.635	0°–1°		VD
14349, Middleton, Conn. with muscovite	1.580	1.635	0°–5°		MD
Alurgite 93915, St. Marcel, Italy		1.607	0°		none
Phlogopite R4463, Masham, P. Q.		1.59	0°–3°		WD
Zinnwaldite 97374, Amelia, Va.	1.550	1.584	0°		none
Lepidolite R4365, Western Aust., Stevens #14	1.525	1.558	0°		none
Biotite, Avery, N. C., (C. S. Ross)	1.597	1.64	0°–3°		VD
Six layer structure (monoclinic hemihedral) U. S. Geological Survey					
Lepidolite, Stevens #6		1.550	25°–30°	$\parallel$ to (010) (b=5.3Å)	none
Stevens #7 U.S.N.M. 97893		1.562	25°–40°	$\parallel$ to (010) (b=5.3Å)	WD
Stevens #12		1.554	35°	$\parallel$ to 010 (b=5.3Å)	WD
Six layer structure (triclinic holohedral) U.S.N.M.					
Biotite 3675, Sterling, N. Y.	1.59	1.645	0°–3°		WD
46127, with muscovite					VD
Biotite 77436, Ambulawa, Ceylon					VWD
Twenty-four layer structure (triclinic holohedral) U.S.N.M.					
Biotite 77436, Ambulawa, Ceylon		1.64	0°–3°		MD

TABLE XIX

Samples with Mixed Structures.

	α	γ	2V	Degree of Diffuseness
From U.S.N.M.				
Biotite 103149, Varnitskaya Bay, Russia	1.59	1.64	0°–3°	MD
R4451, Houghtonite, Respond, Scotland	1.581	1.63	10°–15°	MD
12291, Vesuvius, Italy		1.585	0°–3°	MD
83775, Custer, S. D., with muscovite				WD
11852, Yena Gori, Japan	1.585	1.625	1°–3°	VD
Phlogopite C3686, Sparta, N. Y.				M.D.
R7115, Uhlen Snarum, Norway		1.58	5°–10°	completely D
Campbell Quarry Texas, Md.		1.59	8°–12°	M.D.

From U. S. Geological Survey:
Biotite Franklin, N.C., with muscovite   V.D.
        (C. S. Ross)
        Amelia, Va. (Miss Glass)   1.64   2°–4°   M.D.
From Columbia University:
Biotite Moravia   1.59   0°–3°   WD.
        Larchmont Manor, N. Y.   1.586   1.64   0°–3°   VD
        Tyrol   1.59   3°–7°   MD

TABLE XX

Summary of Observations on Analyzed Lepidolites.

| | Six fold Coordination | | | Structure | Orientation of Plane |
	Al	Li	Σ	Type	of O.A. and 2V
1	1.59	0.73	2.48	Muscovite	⊥ to (010) (b=9.0Å) 38°–40°
2	1.55	0.95	2.54		wavy extinction
3	1.55	1.00	2.60		distorted
4	1.54	1.02	2.58	Too fine grained for study	interference
5	1.51	1.07	2.63		figures
6	1.32	1.36	2.73	6 layer monoclinic	‖ to (010) (b=5.3Å) 25°–30°
7	1.30	1.39	2.86	6 layer monoclinic	‖ to (010) (b=5.3Å) 25°–40°
8	1.35	1.35	2.71	Single layer	‖ to (010) (b=9.0Å) 30°–40°
9	1.36	1.44	2.81	Single layer	‖ to (010) (b=9.0Å) 55°–58°
10	1.10	1.50	2.94	Single layer	‖ to (010) (b=9.0Å) 30°
11	1.35	1.50	2.85	None available	
12	1.31	1.52	2.85	6 layer monoclinic	‖ to (010) (b=5.3Å) 35°
13	1.30	1.56	2.91	Single layer	‖ to (010) (b=9.0Å) 25°–30°
14	1.25	1.62	2.94	3 layer hexagonal	uniaxial
15	1.11	1.68	2.95	Single layer	‖ to (010) (b=9.0Å) 45°
16	1.05	1.85	2.98	Single layer	‖ to (010) (b=9.0Å) 45°
17	0.98	1.94	2.97	Single layer	‖ to (010) (b=9.0Å) 40°

Nineteen of the samples studied were muscovites and all these had the same two layer monoclinic structure. This structure was also shown by the lepidolite sample that approached closest to muscovite in composition and by the analyzed alurgite from California. The optic axial angles (2V) of all the specimens were between 34° and 50° and the plane of the optic axes was perpendicular to (010) in every case.

Forty-five of the remaining seventy-eight biotite-like (octophyllite) micas have the single layer monoclinic structure. They include many phlogopites and seven of the analyzed lepidolites as well as several zinnwaldites. The iron contents of the biotites vary over wide limits as shown by the value of the maximum refractive index and by the presence of such varieties as anomite, cryophyllite, and lepidomelane. The plane of the optic axes was parallel to (010) in all of the samples tested, except

one—phlogopite No. 82459. The optic axial angles of the biotites and phlogopites were very small. Lithium-bearing members, on the other hand, had optic axial angles in the same region as did the muscovites, namely 25–60°.

The single layer structure is often a component present in the mixed type structures given by the thirteen specimens listed in Table XIX. The optic axial angle of all these micas was found to be small.

The five unusual types of structures described earlier in the paper are represented among the remaining twenty specimens examined. Eight of these had the rhombohedral enantiomorphic hemihedral structure. Several of these are strictly uniaxial even in a conoscope with low divergence of the illumination. However, others show a small opening of the interference figure. All give some diffuse scattering, the significance of which will be discussed later. There is no doubt but that the hexagonal description is accurate as a limiting case. This three layer structure was found for a wide variety of compositions including an analyzed lepidolite. The four biotite samples were very darkly colored and had a high maximum index of refraction, which suggests that they had a high iron content.

Five specimens have the two layer monoclinic structure related to that of muscovite but differing from it in the absence of $(0kl)$, l odd reflections. There were three examples of each of the six layer structures and a single case of the twenty-four layer structure.

General Discussion

Three questions naturally come to the fore. What are the factors determining the polymorphism of the micas? What are the relationships between optical properties and structure? In what manner does diffuse scattering arise?

Before addressing any of these, attention should be called to several papers by A. N. Winchell.[12] He recognized a group distinction among the micas which he summarized in the terms heptaphyllite and octophyllite. These terms simply mean that seven and eight positive ions, respectively, are present for twelve negative ions. Muscovite is the type heptaphyllite mica having the formula $[KAl_2AlSi_3O_{10}(OH, F)_2]$ and phlogopite the type octophyllite mica $[KMg_3AlSi_3O_{10}(OH, F)_2]$. This distinction is entirely consistent with the present and previously published information on the mica structures. Another way of expressing it is that micas related to muscovite (heptaphyllites) have only two-thirds

[12] *Am. Jour. Sci.*, (V), **9**, 415 (1925); *Am. Mineral.*, **17**, 551 (1932); **20**, 773 (1935).

of the positions with octahedral coordination relative to oxygen filled while phlogopite (octophyllite) has all such positions filled. Finally, Winchell has made two further statements of use here: "It is important to note that no evidence of crystal solubility between octophyllite and heptaphyllite has been found; on the contrary any good analysis belongs definitely to one or the other, and not to both." "Also certain lithia micas are reported to be triclinic, while others (even in the same rock) seem to be monoclinic. Apparently these micas are dimorphous, and that condition would doubtless entail variations in optical properties, the extent and character of which are at present unknown."

Muscovite in accord with Winchell's concept was found to be invariant in structure and none of the other micas had the same structure. The most characteristic feature of the structure is that it is distorted from the ideal as shown by the presence of reflections from (06l) with l odd. The exact character of the distortion is not known but it undoubtedly is the factor that leads to a unique requirement on the successive stacking of layers. In other words, muscovite has a unique structure because of its distorted layer while the biotites (octophyllites) have variable structures because their layers are symmetrical. The distortion of the layer in muscovite is a result of incomplete filling of the octahedral positions. Thus some octahedral edges will be differently surrounded than others and there will be changes of the type predicted by Pauling's coordination theory. In the biotites (octophyllites) all octahedral positions are filled and the octahedral edges are equivalent.

The distortion of the muscovite layer also probably contributes to the partial birefringence in the cleavage plane and thus increases the optic axial angle. It is apparently for this reason that the partial birefringences $(\gamma - \beta)$ of muscovites are greater than those of other micas.

Results obtained from the lepidolites analyzed by Stevens as summarized in Table XX serve to illustrate the limited solid solutions of muscovite and lepidolite. In Table XX, Σ is the number of atoms having octahedral coordination for every twelve negative ions in a mica; it should be 2 for muscovite (heptaphyllite) and 3 for polylithionite (octophyllite). Sample 1 having $\Sigma = 2.48$ still has the muscovite structure and it is tantalizing to think that samples 2 to 5 owe their poor crystal development to their close approach to the limit of the lepidolite solid solution in muscovite. Samples 6 to 17 show three different structures without evident correlation with composition. These can be considered as solid solutions of muscovite in polylithionite, or better as lithium micas in which more than 11/12 ($\Sigma = 2.75$) of the octahedral positions are filled.

The six layer monoclinic structure is reported in the tables as only being observed for lepidolites and it thus might be thought to be peculiar to them. However, at least two of the mixed types of Table XIX appear to contain a part of this structure type and the absence of a biotite or phlogopite representative appears accidental. The structure is most interesting in that it alone of all the types found, effects an interchange of the usual a- and b-axes. In Table XX it would appear that the optic orientation for this structure is similar to that of the single layer and three layer structure. Actually, it is more comparable with muscovite as represented by sample 1 on account of the interchange of axes. The optic axial angles of the six layer, one layer, and muscovite types of lepidolite are all of the same magnitude as that of muscovite. However, this is really a result of the low birefringence $(\gamma - \alpha)$, the partial birefringence $(\gamma - \beta)$ being about two-thirds to one-half that of muscovite.

While the six layer and single layer lepidolites cannot be distinguished optically, the three layer hexagonal structure is immediately evident. This particular sample (Stevens #14, U.S.N.M. R4365) is a very large sheet from Londonderry in Western Australia. The sheet is predominantly uniaxial but in a few parts the optic axes (2V) open up to 20–40°. These parts upon examination by x-ray diffraction are found to have the single layer structure. If the change is to be accounted for by composition, then it is varying on a small scale and the composite nature of the analyzed material would obscure any correlation between structure and composition. A similar situation was encountered in a zinnwaldite sheet from Amelia, Va., that was kindly supplied by Miss J. J. Glass of the U. S. Geological survey. The optic axial angle (2V) of different parts of the sheet varied from uniaxial to 25°. A uniaxial part had the three layer structure while mixed structure types combining the single layer and three layer structures were found in two of the biaxial parts.

The six layer monoclinic structure is rather analogous to the nacrite structure, as was pointed out in the structure analysis. In fact, the distinction between the various mica structures is more pronounced than that between the kaolin minerals, kaolinite, dickite and nacrite. Absence of appreciable variation of composition among the kaolin minerals made it possible to interpret the optical properties with more certitude than was the case for the micas. In a sense, however, the presence of a uniaxial lepidolite is an indication of polymorphism among the micas.

The truly hexagonal three layer structure is by no means unusual and in fact it occurred with about one-fifth the frequency of the predominant single layer structure among the biotites (octophyllites). The six layer monoclinic structure is related to it in a sense that it too has three-fold screw axes even though these are eliminated as symmetry

operations of the space group by the glide reflection plane. In fact the hexagonal structure can be considered as a combination of two $C_3{}^2-C3_1$ or $C_3{}^3-C3_2$ subgroups with two-fold axes normal to the hexagonal axis (note I.T.D.C.S.) while the six layer monoclinic structure combines either of the same groups with a glide reflection plane with a glide component along the three-fold screw axis. As pointed out before this is of most interest in that it forms an unclosed group of operations.

Remaining structure types are the two layer monoclinic, the six layer triclinic, and the twenty-four layer triclinic. The triclinic ones are of interest in that they give a summary answer to the question of the possible existence of a triclinic mica. As a group they are a motley array without apparent interrelationship except that they are predominantly biotites with probably a high iron content. However, each structure is characterized by having centers of symmetry, an element of symmetry which is absent for the three lepidolite structures.

Good evidence that these three structures are probably related was found in an entirely accidental manner. The crystal taken from the Ambulawa, Ceylon, biotite specimen was among the first examined and it showed the twenty-four layer structure which was merely appreciated as being complex at the time. Later, when a closer examination was to be made, a second crystal from the same specimen was accidentally selected. It proved to have the six layer triclinic structure.

The Ambulawa, Ceylon, specimen which is marked a thoranite-bearing pegmatite, is shown in Fig. 8. Structures of various crystals are indicated in the accompanying diagram (Fig. 8b). It is to be noted that only
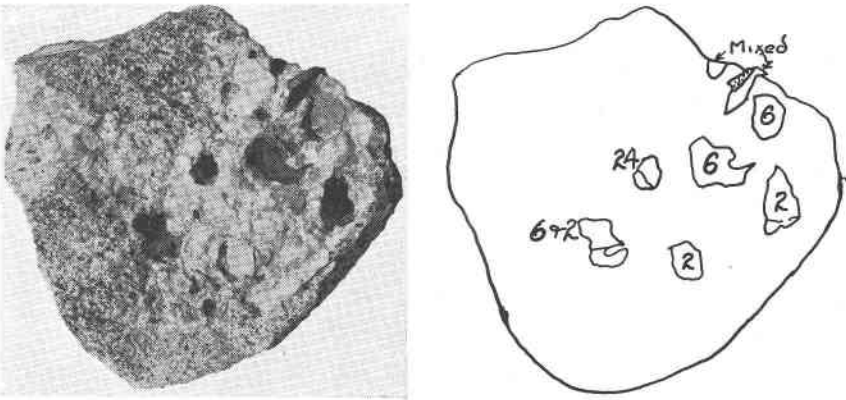

FIG. 8a. Biotite specimen from thoranite-bearing pegmatite, Ambulawa, Ceylon.
FIG. 8b. Drawing of crystals in specimen with indicated layer multiplicities in structures.

two layer monoclinic and six and twenty-four layer triclinic structures are represented, together with mixtures of these. The crystals appear to be closely similar and they probably do not vary appreciably in composition. It would seem therefore that whatever factors determine the structures, composition probably being important, operate for all cases.

The only phlogopite specimen, No. 78218, having one of these structures, is not typical. It is weathered as shown by poor coherence of the cleavage sheets and absence of an interference figure. Moreover, the surface is too drusy for use on the total reflectometer and there are a tremendous number of acicular inclusions.

In general the partial birefringence $(\gamma - \beta)$ of the octophyllite micas other than the lepidolites is so low that the optical character is probably determined more by variation in composition than by structure. The three layer hexagonal micas are closely uniaxial, but so are representatives of the other structures.

A number of specimens were examined, in some of which biotite crystals were included in muscovite and in others muscovite was zoned with lepidolite. In none of these did the biotite or lepidolite take up the muscovite structure. In fact the octophyllite parts of the seven specimens examined afforded examples of four structure types while the muscovite was invariant. Moreover, crystallographic orientations were not the same for the component crystals but rather had other simple relationships.

MIXED STRUCTURES AND RELATIONSHIP OF DIFFUSE SCATTERING OF X-RADIATION TO STRUCTURE

It was mentioned that portions of the zinnwaldite specimen from Amelia, Va., and lepidolite R4365 were mixtures of the single layer and three layer structures. Mixtures of a more complex nature and involving other structures were observed for a number of samples which are listed in Table XX. Since the diffraction photographs are difficult to analyze correctly, no attempt was made to determine the exact type of mixing. The three samples from Columbia University were selected for study on account of their close approach to uniaxial character, this being a qualitative criterion for some structure other than the single layer one.

Different components in a mixed structure maintain parallel orientations, except for variation in the c-axis. Thus the orthohexagonal b-axis of the three layer component in zinnwaldite from Amelia, Va., is parallel to the b-axis of the monoclinic part.

Appreciable development of diffuse scattering along $(h_a k_a l)$, $k \neq n \times 3$, curves was noted on Weissenberg photographs of all samples with mixed structures. Such scattering was also observed for many other micas

examined as indicated in Tables XVI and XVIII, but, significantly, was
not found for any of the muscovites. The phenomenon was first noted by
Mauguin[2] who, without detailed knowledge of the structures, concluded
that it was a result of some type of randomness in positions of the heavy
ions. Others have observed similar scattering from various layer silicate
minerals; among the most recent being Hutton and Fankuchen in their
work on stilpnomelane.[13] A probable explanation of the effect was given
in the paper on the structures of vermiculites[14] and elaborated in the
more recent work on cronstedite.[15] Both of these minerals as well as the
chlorites show pronounced development of the general scattering. The
work on the micas focuses attention on several factors that merit dis-
cussion.

The concept of a mosaic crystal was introduced by C. G. Darwin[16]
in his classical work on diffraction of x-rays by crystals. He demon-
strated that the observed intensities of x-ray diffraction maxima re-
quired crystals to consist of many small elements of volume deviating
slightly from perfect alignment. According to this concept a mica crystal
would consist of parts each of which was a perfect crystal in itself but
which scattered x-rays independent of neighboring parts except insofar
as they form a screen. The total reflection is the summation of the x-rays
scattered from the different parts, but one part does not give inter-
ference with another. Magnitudes of the perfect volumes are unknown
and in fact the whole phenomenon has not been very susceptible of
study.

In micas, as in other layer minerals, the diffuse scattering is restricted
to those Weissenberg curves along which the h and k indices are constant
and the k index not a multiple of three, (h_ak_bl), $k_b \neq n \times 3$. Several typical
Weissenberg goniometer photographs taken with the crystal rotating
about the a-axis, or pseudo a-axis, are shown in Fig. 4. The diffuse scat-
tering is always associated with the strong reflections along a curve. In
this connection it is interesting to compare the diffuse scattering from
phlogopite R7117 and biotite 11852, photographs of which are repro-
duced in Fig. 4c and 4e, respectively. The first closely resembles the usual
pattern of a two layer biotite while the second is related to the photo-
graphs of the single layer and others.

Laue photographs of micas taken with the incident x-ray beam nor-
mal to the cleavage plane show radial streaks that usually have been ex-
plained as "asterism." Such streaks, which are illustrated by Fig. 9, are

[13] *Mineral. Mag.*, **25**, 172 (1938).
[14] Hendricks, S. B., and Jefferson, M. E., *Am. Mineral.*, **23**, 851 (1938).
[15] Hendricks, S. B., *Am. Mineral.*, **24**, 529 (1939).
[16] *Phil. Mag.*, (6), **27**, 325 (1914).

analogous to the continuous Weissenberg curves. Both can be explained in terms of constant h and k indices with an apparently continuous variation of the l index. Qualitatively the entire effect appears to involve a variable length in the stacking of the mica layers that leaves those planes with the k index a multiple of three undisturbed.

Inspection of the various drawings and tables of coordinations will perhaps make it evident that translation of one-half of a mica layer by $nb/3$ with respect to the other half leaves the layer unchanged but results in a change of the relationship of successive layers. This is really the factor that permits the polymorphism of the octophyllite micas. Now if this process is carried out in a random instead of a regular manner there will be no definite c periodicity unless the k index is a multiple of three, in which case the periodicity is that of a single layer. As a result diffuse scattering of the observed type will necessarily appear, and its intensity will depend upon the number of the random shifts.

In the structure analysis of dickite,[17] pyrophyllite, and talc[18] it was found that while intensities of reflections from (hkl), $k = n \times 3$, could be explained, those from (hkl), $k \neq n \times 3$, could not. The explanation advanced was that random shift of one layer with respect to another by $nb/3$ within an element of a crystal mosaic introduced an indefinite shift of phase. In the micas, however, as seen above, calculated intensities in agreement with observed values can be found for (hkl), $k \neq n \times 3$ reflections. It is necessary, therefore, to assume that many elements of a mosaic in a mica crystal showing a well developed structure are perfectly regular and any diffuse scattering is due to random shifts in a limited number of the mosaic elements. Similarly in dickite, pyrophyllite and talc the majority of the elements would have at least one random displacement and none would have many, since no diffuse scattering is observed.

Mica crystals having the single layer structure, for instance might consist of perfect mosaic elements and show no diffuse scattering, or a sufficiently large number of the mosaic elements might have many random elements leading to completely diffuse (hkl), $k \neq n \times 3$ reflections. The presence of mixed structures further serves to support these concepts in that they indicate that different parts of the crystal mosaic can vary in structure.

In the end it is all too evident that the first question has not been answered. What are the factors determining the polymorphism of the micas? Surely it is most surprising that they have fixed structures at all.

[17] Hendricks, S. B., *Am. Mineral.*, **23**, 295 (1938).
[18] Hendricks, S. B., *Zeits. Krist.*, **76**, 211 (1930).

FIG. 9. Laue photographs with the *x*-ray beam approximately normal to the plane of micaceous cleavage. Symmetry planes are indicated by *M*. All photographs were taken with the same crystal to plate distance and peak voltage.
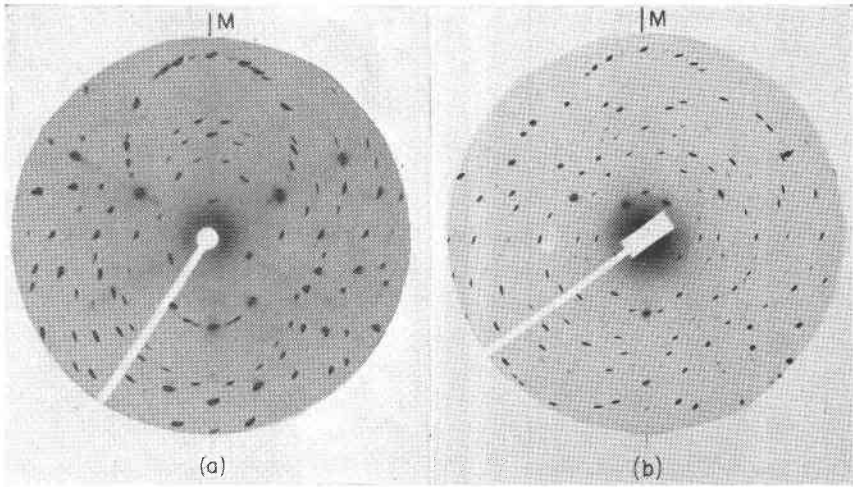
a. Single layer monoclinic hemihedral phlogopite.
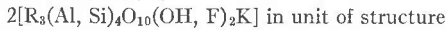*b*. Muscovite, two layer monoclinic holohedral.
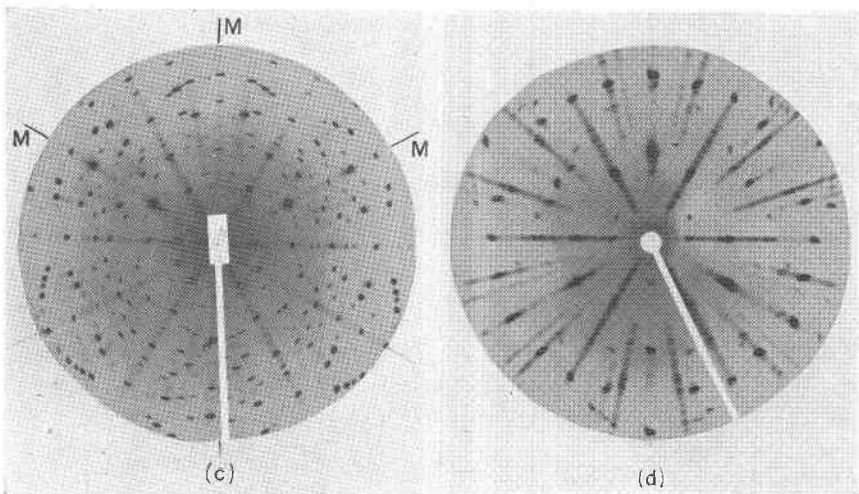
c. Three layer rhombohedral enantiomorphic hemihedral lepidolite. Note radial streaks.
d. Twenty-four layer triclinic holohedral biotite.

SUMMARY

Seven different crystalline modifications were discovered among one hundred specimens of mica that were examined by x-ray diffraction methods. Constants of these various forms and their frequency of occurrence are:

Single layer monoclinic hemihedral (45)

$2[R_3(Al, Si)_4O_{10}(OH, F)_2K]$ in unit of structure
$R = Mg^{++}, Fe^{++}, Fe^{+++}, Li^+, Ti^{++++}$, etc.
$a = 5.3\text{Å}$ $c_0 = 10.2\text{Å}$ Sp. G. $C_s^3 - Cm$
$b = 9.2\text{Å}$ $\beta = 100°$

(A. C.) Atomic Coordinates, Table I
(Struc.) Structure, Fig. 1.
(Photo.) X-ray diffraction patterns, Figs. 4a, b, c, h, 9a.

Two layer monoclinic holohedral, muscovite type (21)
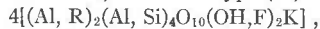
$4[(Al, R)_2(Al, Si)_4O_{10}(OH,F)_2K]$,
$a = 5.2\text{Å}$ $c_0 = 20.0\text{Å}$ Sp. G. $C_{2h}^6 - C2/c$
$b = 9.0\text{Å}$ $\beta = 95° \ 30'$

(A. C.) Table V, (Struc.) Figs. 1b, 3b.
(Photo.) 4d, 9b.

Two layer monoclinic holohedral, octophyllite type (5)
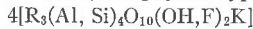
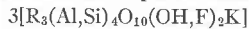$4[R_3(Al, Si)_4O_{10}(OH,F)_2K]$
$a = 5.3\text{Å}$ $c_0 = 20.2\text{Å}$ Sp. G. $C_{2h}^6 - C \ 2/c$
$b = 9.2\text{Å}$ $\beta = 95°$

(A. C.) Table V, (Struc.) Fig. 3a.

Three layer rhombohedral enantiomorphic hemihedral (8)

$3[R_3(Al,Si)_4O_{10}(OH,F)_2K]$
$a = 5.3\text{Å}$ $c_0 = 30.0\text{Å}$ Sp. G. $D_3^3 - C3_1 12$ or $D_3^5 - C3_2 12$

(A. C.) Table VIII, (Struc.) Fig. 5b. (Photo.) 4f, 9c.
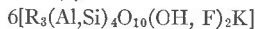
Six layer monoclinic hemihedral (3)
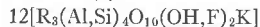
$12[R_3(Al,Si)_4O_{10}(OH,F)_2K]$
$a = 5.3\text{Å}$ $c = 60.0\text{Å}$ Sp. G. $C_s^4 - Cc$
$b = 9.2\text{Å}$ $\beta = 90°$

(A.C.) Table X, (Struc.) Fig. 6., (Photo.) 4g.

Six layer triclinic holohedral (3)

$6[R_3(Al,Si)_4O_{10}(OH, F)_2K]$
$a = 5.3\text{Å}$ $\alpha = 90°$ Sp. G. $C_i^1 - P\bar{1}$
$b = 5.3\text{Å}$ $\beta = 90°$
$c = 60.0\text{Å}$ $\gamma = 120°$

(A.C.) Table XIII, (Struc.) Fig. 7, (Photo.) 4i

Twenty-four layer triclinic holohedral (1)

$24[R_3(Al,Si)_4O_{10}(OH,F)_2K]$
$a = 5.3\text{Å}$ $\alpha = 90°$ Sp. G. $C_i^1 - P\bar{1}$.
$b = 5.3\text{Å}$ $\beta = 90°$
$c = 240.0\text{Å}$ $\gamma = 120°$

(Photo.) 4j, 9d. Structure not determined.

Mixtures (13) of the various structures were found and a general explanation is given for the diffuse scattering of x-rays in some crystal zones. Underlying reasons are given for Winchell's successful grouping of micas as heptaphyllite, or muscovite-like, and octophyllite, or phlogopite-, lepidolite-, biotite-, etc., like.

The general reader and mineral collector will perhaps find the part of the paper after "Optical Properties etc." of most interest. For his use it can be stated that two triclinic, four monoclinic, and one hexagonal modification of mica were discovered. There is some correlation between crystal optics and structure, particularly for lepidolites.